JOURNAL OF SOLID STATE CHEMISTRY 45, 51–62 (1982)

Photoluminescence and Electroluminescence in Graded Cadmium Sulfoselenide Electrodes: Applications to Photoelectrochemical Cells

MICHAEL K. CARPENTER, HOLGER H. STRECKERT, AND ARTHUR B. ELLIS*

Department of Chemistry, University of Wisconsin–Madison, Madison, Wisconsin 53706

Received April 29, 1982

Inhomogeneous samples of *n*-type CdS_xSe_{1-x} ($0 \leq x < 1$) were prepared by vapor-phase diffusion of S into a single-crystal CdSe substrate. Characterization of the samples by Auger electron spectroscopy (AES)/Ar ion sputter etching reveals that S has substituted for Se in the lattice to produce a graded region: The depth profile analysis indicates that from a composition with x nearly unity at the surface, x monotonically declines to zero over a distance of ~1 μm. Correspondingly, the band gap energy diminishes from ~2.4 eV for the CdS-like composition to ~1.7 eV for CdSe. Photoluminescence (PL) and electroluminescence (EL) from the graded material appear to derive from the luminescence of the CdS_xSe_{1-x} compositions which make up the graded region: Emission from ~500–750 nm matches the spectral region spanned by PL and EL from homogeneous, single-crystal CdS_xSe_{1-x} samples which emit near their band gap energies. A previously established linear correlation between emission maxima (nm) and composition in homogeneous CdS_xSe_{1-x} samples provides a spatial probe of electron-hole (e^-–h^+) pair recombination in the inhomogeneous material: Regions from which PL and EL originate can be inferred from their spectral distribution in combination with the AES/depth profile data. PL spectra are thus shown to be dependent on excitation wavelength in a manner consistent with relative optical penetration depth. EL spectra are potential dependent and provide evidence that increasingly cathodic potentials shift the spatial origin of EL, on average, nearer to the semiconductor surface. The inhomogeneous samples can be used as photoanodes of photoelectrochemical cells employing aqueous (poly)sulfide electrolyte. Photoaction spectra exhibit their principal onset at ~560 nm, indicating that the S-rich, near-surface region is primarily responsible for photocurrent. This spatial origin of photocurrent is also reflected in the nonuniform quenching of PL accompanying passage of photocurrent from 457.9-nm excitation. With certain assumptions, these quenching properties provide a crude map relating the efficiency of e^-–h^+ pair separation to distance from the semiconductor–electrolyte interface; the correlation indicates that negligible separation occurs beyond ~0.2 μm. Comparisons of these PL and EL properties with those of related graded materials and with homogeneous CdS_xSe_{1-x} samples are discussed.

Introduction

The use of photoelectrochemical cells (PECs) for the direct conversion of optical energy to electricity has attracted considerable interest (*1–4*). Semiconductors, which serve in the dual roles of photoreceptor and electrode, are the key element of the PEC: Upon absorption of ultraband gap photons, electron-hole ($e^- - h^+$) pairs are generated

* Author to whom correspondence should be addressed.

0022-4596/82/130051-12$02.00/0

and separated for photocurrent by an electric field near the semiconductor–electrolyte interface. The zone in which the electric field occurs, the depletion region, thus plays a critical role in the construction of efficient PECs.

Competing with the separation of e^-–h^+ pairs are their nonradiative and radiative recombination. We have recently reported on the use of luminescence as a probe of recombination in several homogeneous, *n*-type semiconductor electrodes. Emission due to a dopant was investigated with samples of Te-doped CdS (CdS : Te) (*5–7*), and edge emission was studied with members of the CdS_xSe_{1-x} ($0 \leq x \leq 1$) series (*8, 9*). Our general finding was that photoluminescence (PL) could be perturbed and electroluminescence (EL) initiated in aqueous electrolytes by interfacial charge-transfer events.

The homogeneous CdS_xSe_{1-x} samples were particularly intriguing in that they exhibited sharp PL and EL spectra (FWHM ~0.05–0.08 eV) whose maxima varied nearly linearly with composition (Eq. (1); (*9, 10*)). This shift in edge emission corresponds

$$\lambda_{max}(\text{nm}) \cong 718-210\,x \qquad (1)$$

to a decline in band gap value with x, from ~2.4 eV for CdS to ~1.7 eV for CdSe (*11–16*).

While characterizing these systems, it occurred to us that the ability of CdS and CdSe to form solid solutions of any composition might be exploited in the preparation of inhomogeneous solids for which Eq. (1) would identify the spatial origin of e^-–h^+ pair recombination. We recently examined the emissive properties of one such material containing a graded region of ~2 μm thickness (*17*). With certain assumptions, we were able to correlate the efficiency of e^-–h^+ pair separation with distance from the semiconductor surface when the semiconductor was used as a PEC electrode.

In this paper we describe the PL and EL properties of a related solid characterized by a substantially smaller graded region of ~1 μm thickness. Like the aforementioned inhomogeneous material, the samples described herein exhibit color-coded emission which provides information on the spatial origin of e^-–h^+ pair recombination. Besides yielding this spatial correlation, the emissive features afford a means for exploring the interrelationship of electronic structure, excited-state decay routes, and PEC properties in these samples.

Experimental

Materials. Graded CdS_xSe_{1-x} samples were prepared from ~5 × 5 × 1-mm, vapor-grown, single-crystal *c* plates of *n*-CdSe (resistivity ~2 ohm-cm; 4-point probe method), obtained from Cleveland Crystals, Inc., Cleveland. In a typical procedure, a CdSe plate was etched in Br_2/MeOH (1 : 10 v/v) and placed in a 6-mm-i.d., 8-mm-o.d. quartz tube (William A. Sales, Ltd., Wheeling, Ill.) with ~0.6 mg of S; the S was purchased from Alfa Products, Danvers, Massachusetts, and was free of metallic impurities to better then 10 ppm. The quartz ampoule was evacuated (~1 Torr), sealed to a volume of ~2 cm^3, and placed in a preheated Lindberg furnace (700°C) for 15 min. After the ampoule was removed from the furnace, one end was contacted by a heat sink to prevent the S from condensing on the crystal. The crystal was then removed and placed in a similar tube with ~1 mg of Cd, which was obtained from Alfa and had <1 ppm of metallic impurities; the tube was evacuated and sealed and again heated at 700°C for 15 min. After its removal from the ampoule, the crystal was mounted as an electrode as described previously (*5*). The preparation of (poly)-sulfide and peroxydisulfate electrolytes has also been described (*5, 6*).

Sample composition. The composition of the graded samples was determined by Au-

ger electron spectroscopy (AES) in conjunction with Ar ion sputter etching. AES data were obtained on a Physical Electronics Model 548 instrument using a 3-keV, 40-μA primary electron beam which was ~200 μm in diameter. Peaks for Cd, S, and Se at 376, 152, and 1315 eV, respectively, were monitored. Sputter etching was conducted using an ~2-mm-diameter beam of 5-keV, 25-mA Ar ions with the vacuum chamber backfilled to $\sim 5 \times 10^{-5}$ Torr with Ar. The sputter rate was determined by masking part of a CdS crystal with stainless steel and sputtering over the interface; subsequently, the step height was determined on a Hacker Model H/I 700 interference microscope from the observed fringe shifts. Comparable sputtering rates for CdS and CdSe have been reported, suggesting that preferential sputtering is not significant in this system (*18*). Capacitance vs potential measurements were obtained at 1 MHz with a Boonton Electronics Model 72BD capacitance meter and a Hewlett–Packard Model 1454 variable power supply. The crystal was etched down to the substrate on one side and ohmically contacted with Ag paint to the sample holder. The opposite crystal surface was only lightly etched (Br_2/MeOH, 1 : 1000 v/v for 2 sec) and contact made to Au dots (~0.025-cm diameter) which had been vacuum deposited using a grid on a Hitachi Ltd. Type HUS-4GB vacuum evaporator. Measurements were made at several depths, exposed by chemical etching, and also on the CdSe substrate.

Optical measurements and PL properties. Uncorrected, front-surface PL spectra were obtained with the Aminco–Bowman spectrophotofluorometer and Ar ion laser setup described previously (*9*); interference filters were used to eliminate laser plasma lines. PL spectra in air were acquired using 457.9- and 514.5-nm excitation by 10X expanding and masking the 2- to 3-mm-diameter laser beam to fill the sample surface; identical intensities (ein/sec measured with a Tektronix radiometer (*9*)) at the two excitation wavelengths were used without changing the sample geometry. PL spectra resulting from excitation of different crystal strata with 457.9-nm light were obtained by the incremental removal of surface material through chemical etching with dilute Br_2/MeOH (1 : 1000, v/v). After each etching the PL spectrum was recorded in roughly the same geometry. For probing lateral inhomogeneity, the laser beam was masked to ~0.5 × 2 mm; the PL spectra resulting from 457.9-nm excitation at various sites on the crystal surface were then obtained by slight variations in the crystal-detection optics geometry.

PEC experiments. PL properties in a PEC were acquired in 1 *M* OH^-/1 *M* S^{2-}/(0.1 *M* S) (poly)sulfide electrolyte using cells and electrochemical equipment previously reported (*9*). Typically, 457.9-nm light was used for excitation and was delivered in both expanded and unexpanded laser beams. PL spectra were recorded while sitting at various potentials without changing the cell geometry. The open-circuit spectra were run before and after in-circuit spectra to demonstrate reproducibility. Complete i–V curves were also obtained in this geometry. Direct measurement of ϕ_x required reassembling the cell outside of the spectrometer, as described previously (*5*). Photoaction spectra were obtained using light from a 300-W tungsten–halogen projector bulb; the lamp's output was monochromatized by passing the light through a McPherson Model 270 0.35-m monochromator equipped with a grating blazed at 500 nm. Lamp intensity as a function of wavelength (460–800 nm) was measured with a flat-filtered EG & G Model 550-1 radiometer (*9*); the radiometer's output was displayed on a Houston Model 2000 x–y recorder and converted to relative einsteins. Photocurrent from a PEC employing the graded electrode and optically transparent 1 *M* OH^-/1 *M* S^{2-} electrolyte was then

measured at −0.3 V vs SCE (output displayed on the Houston recorder) and corrected for the variation in light intensity to generate the photoaction spectrum.

EL spectra. Uncorrected EL spectra were obtained in 5 *M* NaOH/0.1 *M* $K_2S_2O_8$ peroxydisulfate electrolyte by pulsing the electrode between 0.00 V (11 sec) and a potential cathodic of ~−1.0 V (1 sec), while slowly scanning the emission monochromator (12 nm/min), as described previously (*6, 9*).

Results and Discussion

The sections below describe the synthesis and composition of the samples employed in this study, as well as their PL and EL properties. Although this study focuses on graded CdS_xSe_{1-x} samples grown under a particular set of conditions, comparisons with other graded materials (*17*) and with homogeneous CdS_xSe_{1-x} samples (*8, 9*) are made where appropriate.

A. Synthesis and Sample Composition

Relatively narrow zones of inhomogeneity were prepared by short-term, vapor-phase diffusion of S into an etched, single-crystal CdSe substrate (*19–22*). In a typical experiment, CdSe was heated in an evacuated ampoule at 700°C for 15 min, first in the presence of S, then in the presence of Cd. The two-step heat treatment was needed for electrical conductivity as gauged by the sample's performance as an electrode: The untreated and Cd-treated material performed well as electrodes, but with only a S treatment the material appeared to be insulating by this criterion. Even after the heat treatment with Cd, however, evidence for a resistive layer in the material was obtained from capacitance measurements taken over 0–20 V: In contrast to the substrate which exhibited the expected Schottky–Mott behavior (*1*), the exchanged material, sampled at several depths in the inhomogeneous region, gave capacitance values which were independent of applied voltage and ranged from ~20–100 pF. Similar effects were observed in the samples heat-treated for an hour at 700°C (*17*).

The crystallinity of the near-surface region is also of interest but difficult to assess directly. Preservation of crystallinity is implicit in previous studies of related samples (*19–22*). We found evidence for crystallinity in a long-term experiment: A powder prepared from single-crystal CdSe which was heat-treated for 4 days in the presence of S at 700°C subsequently exhibited CdS lines in its X-ray powder pattern (*17*). Although this does not prove the retention of crystallinity under our synthetic conditions, it does suggest that some degree of crystallinity is likely, a conclusion supported by luminescence data (*vide infra*).

Auger electron spectroscopy (AES) was used in conjunction with Ar ion sputter etching to determine a depth profile of the solids' composition; sputter etching was conducted at a rate of ~300 Å/min while monitoring the AES signals of Cd, S, and Se. Figure 1 indicates that the surface contains mainly Cd and S ($X \cong 0.98$) with a small quantity of Se also present. A monotonic decline in S and increase in Se occur over ~1 μm from the surface (~30 min of sputtering), at which point the graded region gives way to the CdSe substrate. A similar depth profile was found using heat-treatment periods of 1 hr with the graded region's depth increased by a factor of ~2 (*17*). The AES data support the notion that S is predominantly substituting for Se in the lattice rather than entering it interstitially: At any of the sputter times of Fig. 1, the fractional S and Se compositions total to roughly unity when each is expressed as a fraction of its maximum AES signal. It should be noted that since S could be driven toward the bulk by the sputtering process, distances culled from Fig. 1 are probably

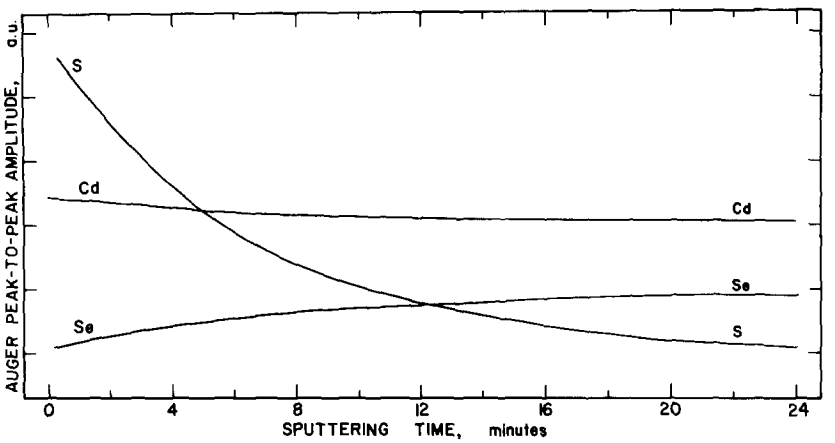

FIG. 1. Auger/depth profile analysis of a graded CdS_xSe_{1-x} sample prepared as described in the text. Sputter etching employed Ar ions and was conducted at a rate of ~300 Å/min. Se was monitored at twice the sensitivity used for Cd and S detection.

best regarded as upper limits (*23*, *24*). That the distances are roughly correct, however, was shown independently by exposing different strata in the graded region using chemical etching; as described below, PL changes accompany this process and, by confining the etching to half of the sample, an estimate of the graded thickness was obtained by measuring step heights with a contacting stylus (*17*).

B. PL Properties

Front-surface, uncorrected PL spectra, obtained in air using 457.9- and 514.5-nm excitation from an Ar ion laser, are shown in Fig. 2 and support the graded nature of

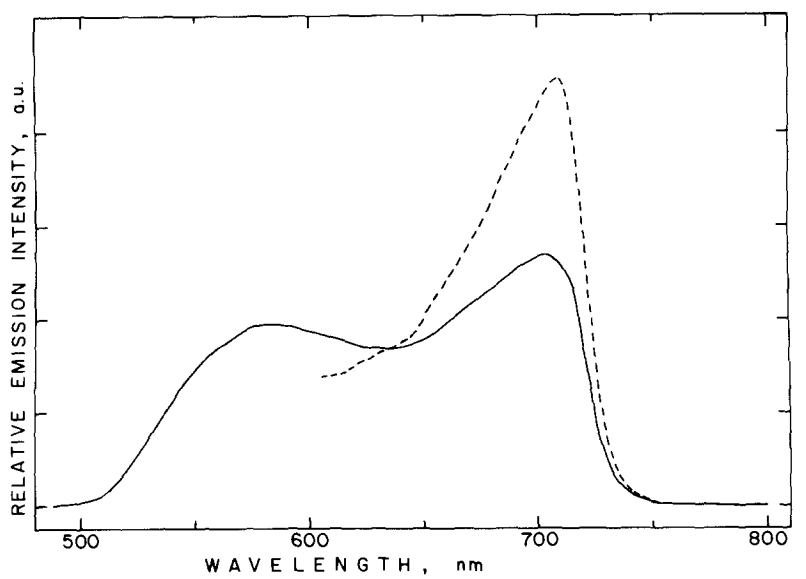

FIG. 2. Uncorrected PL spectra, taken in air, of a graded CdS_xSe_{1-x} sample prepared as described in the text. The entire ~0.15-cm^2 exposed surface area of the sample was uniformly irradiated with ~4 × 10^{-9} ein/sec of 457.9- (——) and 514.5-nm (– – –) excitation from an Ar ion laser; the sample geometry was identical in both experiments.

the material inferred from the AES/sputter etch data of Fig. 1. The range of emitted wavelengths, ~500–750 nm, is consistent with PL contributions from single-crystal CdS_xSe_{1-x} compositions from $x = 0$ to $x \sim 1$ (cf. Eq. (1)). The PL spectra of the graded samples thus appear to derive from the edge emission bands characteristic of the compositions which constitute the graded region. Additional support for this assignment comes from chemical etching experiments which permit various strata to be excited by 457.9-nm excitation: As layers of the material are removed by a Br_2/MeOH etchant, the short-wavelength onset of the PL spectrum red-shifts, consistent with the disappearance of near-surface, S-rich compositions. Similar etching effects on PL spectra were reported for related solids at 77K (*21*). We should point out that although the PL spectra of our samples seem to be dominated by edge emission, we cannot rigorously exclude small contributions from, e.g., impurity-based transitions, and in some samples we did observe weak PL at $\lambda > 750$ nm. Also worth mentioning are modest variations in PL spectral distributions between 500 and 750 nm for the various samples examined; Fig. 2 is a representative spectrum.

Further support for the gradation in composition comes from the dependence of the PL spectral distribution data of Fig. 2 on excitation wavelength. Because 457.9-nm light lies above the band gaps of all CdS_xSe_{1-x} compositions, it should have a shorter penetration depth than 514.5-nm light, which lies on the CdS-absorption edge; we estimate the absorptivity, α, for 457.9-nm light as $\sim 10^5$ cm^{-1} for all sulfoselenide compositions, whereas α is $\sim 10^2$–10^3 cm^{-1} at 514.5 nm for CdS (*14, 16*). Consequently, for the same incident intensity, we expect PL from more deeply penetrating 514.5-nm excitation to have greater contributions from the Se-rich compositions than PL from 457.9-nm irradiation. The enhanced intensity in the low-energy tail of the PL band from 514.5-nm excitation bears out this expectation. Of course, the discrepancy in PL spectra reflects not only the difference in penetration depth, but also the relative efficiencies with which the various CdS_xSe_{1-x} compositions emit.

Figure 2 reveals that emission at $\lambda > 700$ nm, characteristic of Se-rich compositions, is observed with 457.9-nm excitation. Since the AES data indicate that the thickness of the graded region exceeds the penetration depth of the incident light, this result suggests that such processes as e^-–h^+ ambipolar diffusion and/or excited-state energy transfer may play significant roles in this system. A similar observation made for samples prepared by the hour-long heat treatment indicates that these processes might involve distances on the order of a micron (*17*).

An alternative explanation involves the possible existence of lateral inhomogeneity in the graded samples. The existence of CdSe "pinholes," for example, could account for the observed PL properties. Evidence for some lateral inhomogeneity is found in PL measurements: Excitation at 457.9 nm with a masked laser beam (~1-mm^2 area) at various positions on the crystal surface reveals some variation in the PL spectra. To illustrate, the ratio of the intensity at 550 nm to that at 700 nm varied from ~0.7 to 2.1 over eight excitation sites; in contrast, the PL spectra of samples which were heat-treated for an hour typically exhibited variations in the spectral distribution of $\lesssim 15\%$. Although we sought to minimize lateral inhomogeneity by confining our studies to regions where only small differences in PL properties were evident, even in these zones some inhomogeneity could be present. The possible existence of lateral inhomogeneity must be kept in mind, since it could influence many of the results described below.

C. PL Properties in a PEC

Homogeneous, *n*-type CdS_xSe_{1-x} sam-

ples have been used for some time as photoanodes of PECs employing aqueous polysulfide electrolytes; the oxidation and reduction of polysulfide species represent offsetting half-reactions which permit the sustained conversion of optical energy to electrical energy (*25, 26*). We recently reported on the PL properties of homogeneous CdS_xSe_{1-x} samples employed as photoelectrodes in such PECs (*8, 9*). We found that the passage of photocurrent quenched the PL intensity of these samples but did not perturb the spectral distribution. An expression which related the ratio of open-circuit to in-circuit radiative quantum efficiency (ϕ_{r_0} and ϕ_{r_i}, respectively) from monochromatic excitation for these samples to the photocurrent quantum efficiency, ϕ_x, is given by Eq. (2); ϕ_x and ϕ_{r_i} are measured at the same in-circuit potential.

$$\frac{\phi_{r_0}}{\phi_{r_i}} = \frac{1}{1 - \phi_x}. \qquad (2)$$

The same reasonably good fit of PL data to Eq. (2) for CdS_xSe_{1-x}-based PECs has also been observed with homogeneous semiconductor electrodes whose emission is based on dopants such as CdS : Te (*27*) and ZnO : Cu (*28*). A simple interpretation of Eq. (2) is that the fraction of $e^- - h^+$ pairs separated by the depletion region to produce photocurrent is the fraction prevented from recombining and the fraction by which PL intensity is quenched. Equation (2) is readily derived by assuming that the ratio of radiatively to nonradiatively recombining $e^- - h^+$ pairs is unaffected by changes in potential which serve simply to divert various fractions of $e^- - h^+$ pairs to the production of photocurrent (*27*).

In extending these studies to the graded materials, we initially investigated their ability to serve as electrodes. The inset of Fig. 3 displays a typical i–V curve for such an electrode excited with ultraband gap 457.9-nm light in a PEC employing aqueous sulfide electrolyte. These i–V properties correspond to a ϕ_x value of 0.30 at −0.3V vs SCE. Similar i–V curves were obtained in polysulfide electrolyte and yielded a maximum optical to electrical energy con-

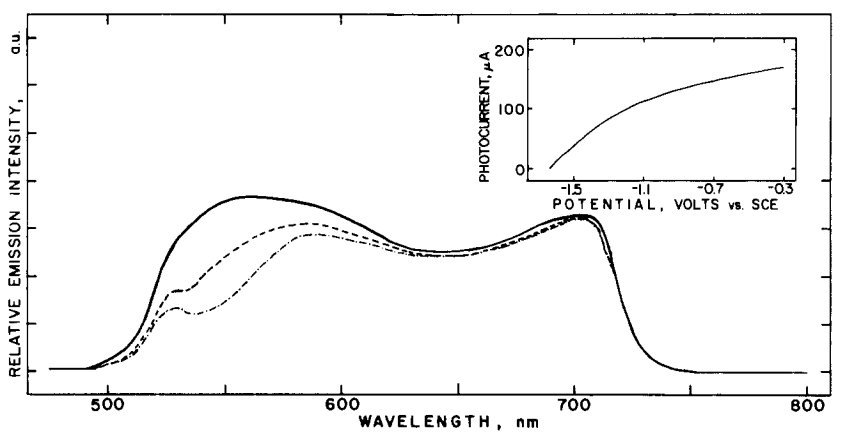

FIG. 3. PL spectra and i–V properties of the graded CdS_xSe_{1-x} sample of Fig. 2. The inset shows i–V properties obtained with 457.9-nm excitation of the electrode when incorporated in a PEC employing 1 *M* OH^-/1 *M* S^{2-} electrolyte. The Ar ion laser beam used for excitation uniformly irradiated the entire ~0.15-cm^2 sample surface area with ~1.6 mW of power. A sweep rate of 10 mV/sec was used and the electrolyte redox potential was −0.71 V vs SCE. Corresponding uncorrected PL spectra obtained at open circuit (——), −1.0 V (– – –), and −0.3 V vs SCE (– · –) are shown in the main panel of the figure. All spectra were taken in an identical sample geometry which differed from that of Fig. 2. Similar data were obtained in 1 *M* OH^-/1 *M* S^{2-}/0.1 *M* S electrolyte.

version efficiency for 457.9-nm light of ~2%. For comparison, graded materials prepared by hour-long heat treatments gave similar output parameters (*17*), while homogeneous CdS_xSe_{1-x} electrodes yielded efficiencies of ~7–12% and near-unity ϕ_x values (*9*).

The central portion of Fig. 3 plots the PL spectrum of the graded electrode at open circuit, −1.0, and −0.3 V vs SCE. In sharp contradistinction to a homogeneous CdS_xSe_{1-x} electrode, *the PL spectral distribution of the inhomogeneous sample is potential dependent:* Passage of photocurrent preferentially quenches the high-energy portion of the PL spectrum which corresponds to S-rich, near-surface regions; the extent of quenching at some wavelengths reaches ~70% between open circuit and −0.3 V vs SCE. By comparison, the PL intensity from the more remote, Se-rich regions suffers far less quenching, typically $\lesssim$5% between open circuit and −0.3 V vs SCE.

Our interpretation of these results is based on the application of the model used for homogeneous electrodes to each composition and region of the inhomogeneous electrode. Thus the use of Eqs. (1) and (2) in conjunction with the data in Figs. 1 and 3 permits a mapping of the fraction of e^-–h^+ pairs separated to yield photocurrent as a function of the distance from the semiconductor surface. To illustrate, PL wavelengths of $\lesssim$550 nm correspond to CdS_xSe_{1-x} compositions of $x \gtrsim 0.8$; to distances of $\lesssim$0.1 μm from the surface; and to e^-–h^+ pair separation efficiencies at −0.3 V vs SCE of up to 70%. The relatively minor quenching for PL wavelengths $\gtrsim$650 nm implies that beyond ~0.2 μm, e^-–h^+ pair separation is very inefficient. The direct ϕ_x measurement of 0.30 at −0.3 V vs SCE is in accord with this interpretation in the sense of being a reasonable value for a material whose various regions contribute from ~0 to 70% of their photogenerated e^-–h^+ pairs to current. The particular importance of the near-surface compositions to photocurrent is also underscored by a photoaction spec-

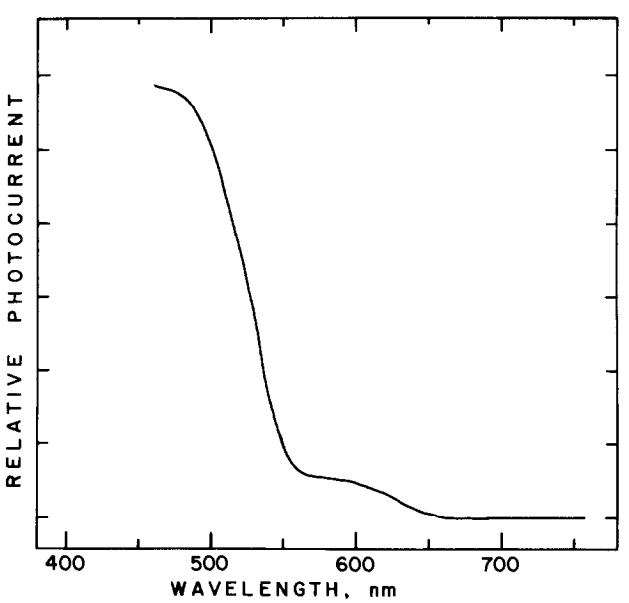

FIG. 4. Photoaction spectrum for a PEC employing the graded CdS_xSe_{1-x} electrode of Figs. 2 and 3 in an optically transparent 1 *M* OH^-/1 *M* S^{2-} electrolyte; the electrode was held at −0.3 V vs. SCE. The plotted values of relative photocurrent have been corrected for variation in light intensity as a function of wavelength.

trum of the material (Fig. 4), which plots relative ϕ_x values vs wavelength. This curve, which rises steeply at ~560 nm, supports the conclusion drawn from Fig. 3 that the near-surface, S-rich compositions are principally responsible for photocurrent. Analogous spatial information from PL data is masked in the homogeneous electrodes, of course, by the spatial independence of the PL spectrum. For such systems, the diminished band bending and e^-–h^+ pair separation efficiency which occur with increasing distance from the semiconductor surface (*1–4, 29*) suggest that their PL quenching properties be treated as a spatially weighted average.

Although the application of the aforementioned model to the graded system is appealingly simple, it must be emphasized that we are making several assumptions regarding material properties. In particular, we are assuming lateral homogeneity, the accuracy of distances extracted from Fig. 1, and the exclusive presence of edge emission in PL spectra. Implicit in our use of Eq. (2) is the assumption on which it rests, viz., that the ratio of radiatively to nonradiatively recombining e^-–h^+ pairs is independent of electrode potential over the potential regime examined. It is noteworthy, however, that even homogeneous electrodes exhibit discrepancies from Eq. (2) (*27*). This is not unexpected given the many factors—optical penetration depth, depletion region width, depth profile of PL intensity, minority carrier diffusion lengths, e.g.—which can influence PL quenching.

Another way to describe the spatial correlation extracted from the PL quenching data is as a map of the effective electric field in the graded sample. For a homogeneous semiconductor this could simply be described as a map of the depletion region. However, the electric field present in graded systems can consist not only of space-charge and applied-voltage contributions, but also of terms based on band-edge and effective-mass gradients, hence its description as an effective electric field (*30, 31*). Although we presently lack a detailed description of the electronic structure of our systems with which to analyze these effects, some related systems have been discussed in connection with the use of a CdSe electrode in a PEC employing polysulfide electrolyte (*18, 32*). Exchange reactions can occur in this system and band diagrams proposed for a composition with CdS on CdSe predict the presence of a barrier in the valence band which would block the passage of holes to the surface; a conduction band barrier preventing passage of electrons into the bulk may also exist. The presence of such barriers might well control the distance over which e^-–h^+ pairs can efficiently be separated to yield photocurrent. In this context, an intriguing feature of the ~0.2-μm depth deduced for efficient e^-–h^+ pair separation is its reduction from the ~0.4-μm value calculated from analogous experiments on the hour-long, heat-treated sample (*17*). These data would be consistent with the creation of a boundary for efficient e^-–h^+ pair separation from barriers in the graded region: As the graded region shrinks, the barriers move nearer to the surface. We are presently preparing graded materials of a broader range of thicknesses to better test this model.

D. EL Properties

EL has been exhibited by a number of *n*-type semiconductor electrodes when employed as dark cathodes in aqueous, alkaline peroxydisulfate electrolyte (*6, 8, 9, 33–36*). The proposed mechanism is given by Eqs. (3)–(5),

$$S_2O_8^{2-} + e^-_{CB} \rightarrow SO_4^{2-} + SO_4^{-}, \quad (3)$$

$$SO_4^{-} \rightarrow SO_4^{2-} + h^+_{VB}, \quad (4)$$

$$e^- + h^+ \rightarrow \text{light}, \quad (5)$$

where e^-_{CB} is an electron in or near the conduction band and h^+_{VB} is a hole in or near the valence band; the key step, Eq. (4), is believed to be the injection of a hole into the valence band by the sulfate radical anion, a

potent oxidizing agent (*33–35*). If, in Eq. (5), the e^- and h^+ are near the band edges, edge emission is observed; if the e^- and/or h^+ reside in an intraband gap state prior to recombination, subband gap emission is produced.

The EL spectra of homogeneous CdS_xSe_{1-x} electrodes are fairly similar to their PL counterparts, indicating that the same emissive excited state is populated in both experiments (*9*). At high resolution, differences in these spectra are observed which are consistent with EL originating, on average, nearer the semiconductor surface than PL. This spatial discrepancy was also found in the hour-long, heat-treated graded electrode (*17*): The EL spectrum was significantly blue-shifted relative to the PL spectrum excited by 457.9-nm light, consistent with greater contributions to the EL spectrum from near-surface, S-rich compositions. For both the graded (hour-long heat treatment) and homogeneous electrodes, EL spectral distributions were essentially independent of the potential used to observe them, typically −1.0 to −1.5 V vs SCE.

The graded samples of this study exhibit EL spectra, which, like their PL counterparts, appear to derive from the edge emission bands of the constituent CdS_xSe_{1-x} compositions. An initial point to be made is that gross lateral inhomogeneities are particularly evident in EL experiments conducted with these samples: Initiation of EL at −1.5 V vs SCE reveals predominantly regions of green emitted light, but some regions of orange emission are seen as well. The EL spectra of Fig. 5 are based on a region which, visually, was homogeneous and emitted green light at −1.6 V vs SCE. Figure 5 demonstrates that EL from these samples, obtained using a pulse technique (*6*), has the unusual property of a potential-dependent spectral distribution: As the potential used to initiate EL is varied from −1.3 to −1.6 V vs SCE, the spectral distribution blue-shifts from the red to the green portion of the spectrum. This spectral shift is reversible over at least several changes in initiation potential and can be viewed directly by the dark-adapted eye, although the red-orange emission at −1.3 V is very weak. As is also the case with the potential-dependent PL spectra, this effect may be of use in display technology.

The color-coded nature of the luminescence permits us to deduce from the Fig. 5 data that as the initiation potential becomes more cathodic, EL originates, on average, nearer the semiconductor–electrolyte interface. One possible explanation for this may involve the concentration of conduction band electrons near the surface available for recombination. At the more anodic potentials, a lower concentration of (near-) surface electrons is expected, permitting an injected hole to diffuse relatively deeply into the semiconductor before recombination occurs; this would lead to the domination of the EL spectrum by contributions from more remote, Se-rich compositions. At the more cathodic potentials, a greater concentration of (near-)surface electrons would enhance the likelihood of recombination in the S-rich region of the electrode. Of course, a detailed discussion of these effects is premature in the absence of, e.g., accurate band structure data. One other feature to be noted in the EL spectra of Fig. 5 is the presence of subband gap emission. Although the prominence of such emission in the EL spectra relative to corresponding PL spectra suggests the involvement of surface states, the origin of this emission remains to be established.

Conclusion

The graded samples described above amply demonstrate, we feel, the viability of using inhomogeneous electrodes to probe spatial aspects of e^-–h^+ pair recombination through luminescent properties. A particularly important application is the construc-

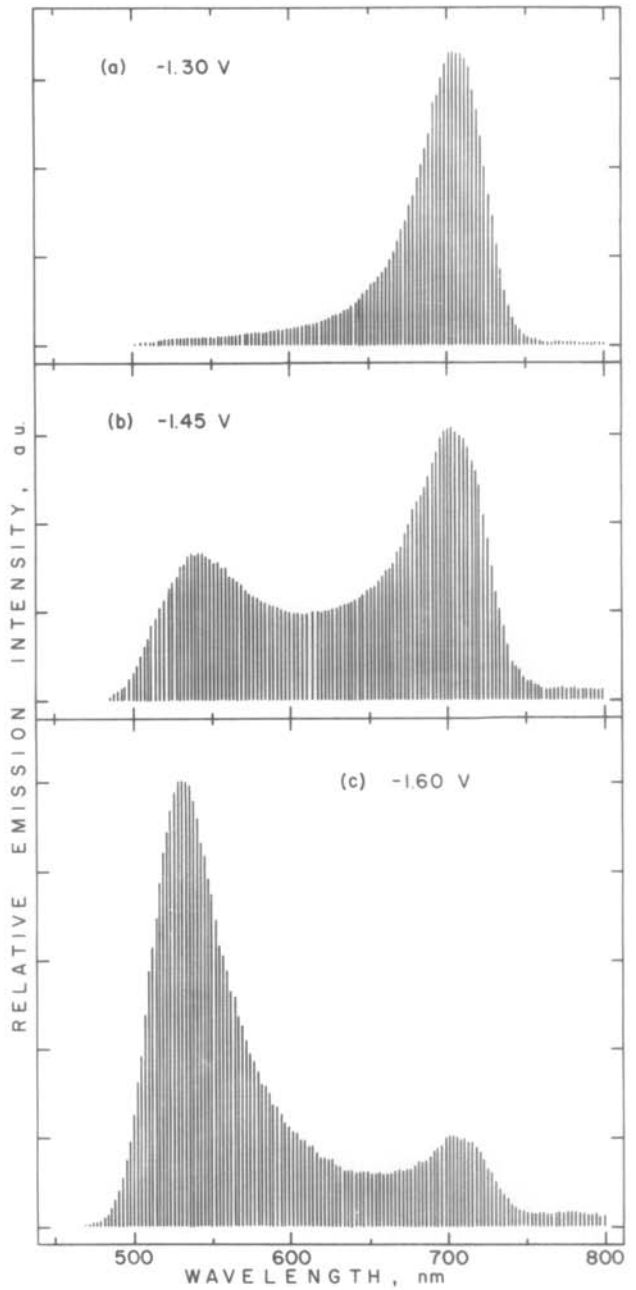

FIG. 5. Uncorrected EL spectra of the graded CdS_xSe_{1-x} electrode of Fig. 1. The series of vertical lines which constitute the EL spectra were obtained in 5 *M* OH^-/0.1 *M* $S_2O_8^{2-}$ electrolyte by repetitively pulsing between 0.00 V (11 sec) and −1.30 V (top panel), −1.45 V (middle panel), or −1.60 V (bottom panel) for 1 sec while scanning the emission monochromator at 12 nm/min. The −1.30-V spectrum was obtained at both the beginning and end of this experiment to demonstrate reproducibility. All spectra were taken in an identical sample geometry; however, the −1.45-V spectrum was taken at twice the sensitivity used to obtain the −1.30- and −1.60-V spectra.

tion, with certain assumptions, of a map relating the efficiency of e^-–h^+ pair separation to distance from the semiconductor surface. Given the crucial role that e^-–h^+ pair recombination plays in the design of efficient PECs, this correlation represents a powerful tool for integrating PEC parameters with spatial features of the semiconductor's electronic structure and excited-state decay properties. The variation in emissive properties with preparative conditions is particularly intriguing and suggests that the study of related graded systems should further clarify the relationships under investigation. Such studies are in progress.

Acknowledgments

This work was generously supported by the Office of Naval Research. A.B.E. gratefully acknowledges support as an Alfred P. Sloan Fellow (1981-3). We thank Dr. Lee Shiozawa and Professors John Wiley, Ferd Williams, and Giorgio Margaritondo for helpful discussions. Dr. Ngoc Tran is thanked for his assistance with the AES measurements.

References

1. A. J. Nozik, *Annu. Rev. Phys. Chem.* **29,** 189 (1978).
2. M. S. Wrighton, *Acc. Chem. Res.* **12,** 303 (1979).
3. A. J. Bard, *Science* **207,** 139 (1980).
4. A. Heller, *Acc. Chem. Res.* **14,** 154 (1981).
5. B. R. Karas and A. B. Ellis, *J. Amer. Chem. Soc.* **102,** 968 (1980).
6. H. H. Streckert, B. R. Karas, D. J. Morano, and A. B. Ellis, *J. Phys. Chem.* **84,** 3232 (1980).
7. B. R. Karas, H. H. Streckert, R. Schreiner, and A. B. Ellis, *J. Amer. Chem. Soc.* **103,** 1648 (1981).
8. H. H. Streckert, J. Tong, and A. B. Ellis, *J. Amer. Chem. Soc.* **104,** 581 (1982).
9. H. H. Streckert, J. Tong, M. K. Carpenter, and A. B. Ellis, *J. Electrochem. Soc.* **129,** 772 (1982).
10. G. Oelgart, R. Stegmann, and L. John, *Phys. Status Solidi A* **59,** 27 (1980).
11. F. L. Pedrotti and D. C. Reynolds, *Phys. Rev.* **127,** 1584 (1962).
12. R. H. Bube, *J. Appl. Phys.* **35,** 586 (1964).
13. Y. S. Park and D. C. Reynolds, *Phys. Rev.* **132,** 2450 (1963).
14. D. Dutton, *Phys. Rev.* **112,** 785 (1958).
15. R. G. Wheeler and J. Dimmock, *Phys. Rev.* **125,** 1805 (1962).
16. R. B. Parsons, W. Wardzynski, and A. D. Yoffe, *Proc. Roy. Soc. London Ser. A* **262,** 120 (1961).
17. H. H. Streckert and A. B. Ellis, *J. Phys. Chem.*, In Press.
18. R. N. Noufi, P. A. Kohl, J. W. Rogers, Jr., J. M. White, and A. J. Bard, *J. Electrochem. Soc.* **126,** 949 (1979).
19. E. T. Handelman and W. Kaiser, *J. Appl. Phys.* **35,** 3519 (1964).
20. H. H. Woodbury and R. B. Hall, *Phys. Rev.* **157,** 641 (1967).
21. H. F. Taylor, V. N. Smiley, W. E. Martin, and S. S. Pawka, *Phys. Rev. B* **5,** 1467 (1972).
22. L. J. Brillson and E. M. Conwell, *J. Appl. Phys.* **45,** 5289 (1974).
23. P. W. Palmberg, *J. Vac. Sci. Technol.* **9,** 160 (1972).
24. D. M. Holloway, *J. Vac. Sci. Technol.* **12,** 392 (1975).
25. A. B. Ellis, S. W. Kaiser, and M. S. Wrighton, *J. Amer. Chem. Soc.* **98,** 6855 (1976).
26. R. N. Noufi, P. A. Kohl, and A. J. Bard, *J. Electrochem. Soc.* **125,** 375 (1978).
27. A. B. Ellis, B. R. Karas, and H. H. Streckert, *Faraday Discuss. Chem. Soc. No. 70,* 165 (1980).
28. A. Fujishima, Y. Maeda, S. Suzuki, and K. Honda, *Chem. Lett.* **1982,** 179.
29. H. Gerischer, *J. Electroanal. Interfacial Electrochem.* **58,** 263 (1975).
30. T. Gora and F. Williams, *Phys. Rev.* **177,** 1179 (1969).
31. L. J. Van Ruyven and F. E. Williams, *Amer. J. Phys.* **35,** 705 (1967).
32. A. Heller, G. P. Schwartz, R. G. Vadimsky, S. Menezes, and B. Miller, *J. Electrochem. Soc.* **125,** 1156 (1978).
33. K. H. Beckmann and R. Memming, *J. Electrochem. Soc.* **116,** 368 (1969).
34. R. Memming, *J. Electrochem. Soc.* **116,** 785 (1969).
35. B. Pettinger, H.-R. Schöppel, and H. Gerischer, *Ber. Bunsenges. Phys. Chem.* **80,** 849 (1976).
36. Y. Nakato, A. Tsumura, and H. Tsubomura, *Chem. Phys. Lett.* **85,** 387 (1982).